

Deconstructing the Failure of Ideal Noise Correction: A Three-Pillar Diagnosis

Chen Feng^{1,*}, Zhuo Zhi², Zhao Huang³, Jiawei Ge⁴, Ling Xiao⁵

Nicu Sebe⁶, Georgios Tzimiropoulos⁴, Ioannis Patras⁴

¹Queen’s University Belfast ²University College London ³University of Aberdeen

⁴Queen Mary University of London ⁵Hokkaido University ⁶University of Trento

Abstract

Statistically consistent methods based on the noise transition matrix (T) offer a theoretically grounded solution to Learning with Noisy Labels (LNL), with guarantees of convergence to the optimal clean-data classifier. In practice, however, these methods are often outperformed by empirical approaches such as sample selection, and this gap is usually attributed to the difficulty of accurately estimating T . The common assumption is that, given a perfect T , noise-correction methods would recover their theoretical advantage. In this work, we put this longstanding hypothesis to a decisive test. We conduct experiments under idealized conditions, providing correction methods with a perfect, oracle transition matrix. Even under these ideal conditions, we observe that these methods still suffer from performance collapse during training. This compellingly demonstrates that the failure is not fundamentally a T -estimation problem, but stems from a more deeply rooted flaw. To explain this behaviour, we provide a unified analysis that links three levels: macroscopic convergence states, microscopic optimisation dynamics, and information-theoretic limits on what can be learned from noisy labels. Together, these results give a formal account of why ideal noise correction fails and offer concrete guidance for designing more reliable methods for learning with noisy labels.

1. Introduction

Learning with noisy labels (LNL) is a fundamental and pervasive challenge in modern machine learning. Label inaccuracies, often arising from human error or automated annotation, can seriously bias model training and weaken generalisation. To address this, a prominent family of solutions, known as *statistically consistent* methods, offers theoretical guarantees of convergence to the optimal classifier one would obtain from clean data. Central to this class is the *noise transition matrix* (T) framework [19, 22, 45],

which explicitly models the label corruption process to enable principled loss correction or risk estimation.

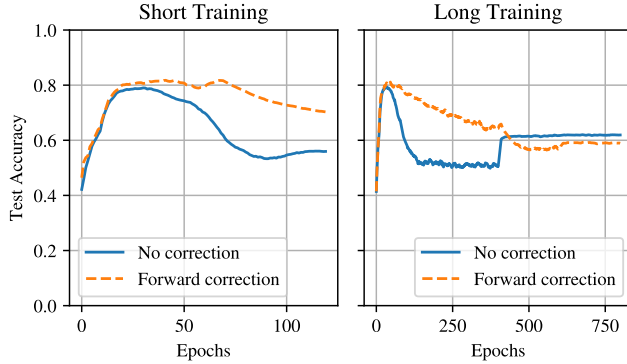
Yet, despite their theoretical elegance, a persistent paradox remains: in practice these principled methods are often outperformed by empirically successful yet *statistically approximate* approaches, such as sample selection [20, 28]. A superficial explanation for this performance gap is that many state-of-the-art sample selection methods are complex hybrid frameworks, integrating powerful techniques such as model ensembling [20, 62], semi-supervised learning [28], and advanced data augmentations [29, 43]. However, these components are conceptually orthogonal to the core LNL setting and could, in principle, be combined with either family of methods.

This shifts the focus to a more dominant hypothesis within the LNL community: the failure of noise correction methods is attributed almost exclusively to the difficulty of accurately estimating the noise transition matrix T [39, 53, 60]. The widely held belief is that, if a sufficiently accurate T were available, this paradox would be resolved and these theoretically motivated methods would regain their expected advantage.

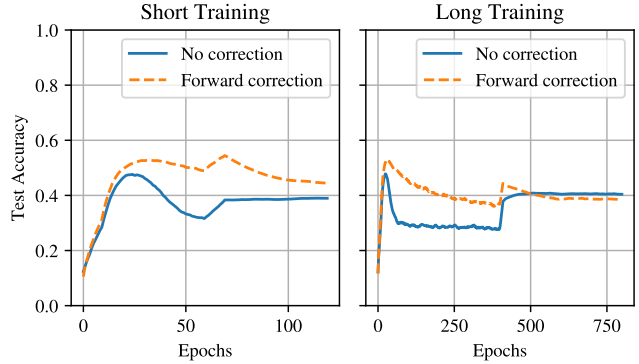
In this work, we put this longstanding hypothesis to a decisive test. We conduct controlled experiments under idealised conditions, providing the correction methods with a perfect, oracle transition matrix. To isolate the core mechanism, our experimental setup is deliberately minimalistic, removing auxiliary components that are often bundled with such methods. The results, shown in Figure 1, challenge the conventional view. Even with a perfect T , Forward Correction (FC) exhibits a pronounced rise-and-fall dynamic and eventually converges to the same poor performance as direct training without any loss correction. This is strong evidence that the failure of noise correction is not fundamentally a problem of estimating T ; instead, it reflects a deeper limitation of the corrected objective itself.

In this paper, we conduct a rigorous investigation to diagnose the root causes of this *ideal tool failure*. Our objective is explicitly *not* to propose yet another correction heuristic, but rather to provide a comprehensive theoretical

*Corresponding author: <https://mrchenfeng.github.io>.



(a) Test accuracy on CIFAR-10 with 50% symmetric noise.



(b) Test accuracy on CIFAR-100 with 50% symmetric noise.

Figure 1. Comparison of test accuracy across different training durations. Even when provided with the ground-truth transition matrix (Oracle T), the model’s performance collapses after an initial peak. Prolonged training sees the correction method’s efficacy degrade, ultimately offering no benefit over the uncorrected baseline.

analysis that systematically explains *why* these principled methods fail even when supplied with perfect information. To this end, our analysis departs from traditional asymptotic bounds and moves beyond common simplifying assumptions such as class-conditional noise (CCN) or deterministic posteriors, so that the conclusions apply to a broad range of practical settings. Our diagnosis is built on three complementary results:

1. A **macroscopic analysis** contrasting the *Ideal Fitted Case* with the *Empirical Overfitted Case* to characterise the final convergence states.
2. A **microscopic analysis** examining the optimisation dynamics and per-sample gradients to expose inherent instabilities.
3. A **fundamental analysis** adopting an information-theoretic view to quantify the unavoidable information loss introduced by the noise corruption process.

Collectively, these findings uncover the mechanisms that drive this paradox and provide the community with a rigorous account of why statistically consistent methods falter, pointing towards design principles for more reliable LNL solutions.

2. Related Work

Noise Transition Matrix (T-Matrix). This paradigm seeks to establish strong statistical foundations, aiming to guarantee *classifier consistency* asymptotically [2, 5–7, 26, 27, 30, 65–67]. Seminal works introduced Forward and Backward Correction to rectify loss or risk using the matrix T [22, 23, 33, 35, 36, 42, 45, 56, 59]. Consequently, the field dedicated extensive effort to the accurate estimation of T , evolving from early *anchor point assumptions* [38, 53] to advanced structure-based techniques (e.g., volume minimization, clusterability [31, 60, 70]). Recently,

attention shifted to the complexity of Instance-Dependent Noise (IDN) [3, 54], though identifying IDN remains generally ill-posed without strong inductive biases [39].

Robust Loss Functions. A parallel theoretical approach focuses on designing inherently tolerant loss functions, such as GCE, MAE, and SCE [18, 50, 68]. Unlike matrix-based methods, these approaches bypass the explicit modeling of the noise process via T , achieving asymptotic Bayes consistency by imposing specific structural constraints, notably the symmetry condition.

Empirically-Driven Sample Selection. These methods prioritize empirical efficacy using heuristics (e.g., the ‘small-loss’ hypothesis) to filter clean samples. Pioneering works like Co-teaching [20, 62] utilized dual networks for cross-filtering. This evolved into a diverse array of filtering and regularization techniques based on prediction confidence, graph consistency, and feature-space topology [8, 11–13, 15, 28, 32, 34, 37, 44, 46–48, 51, 52]. Recent state-of-the-art frameworks further integrate semi-supervised and contrastive learning [9, 10, 24, 28, 29]. While adaptable, they fundamentally rely on the implicit regularization of deep networks rather than formal statistical correction.

3. Problem Setting and Preliminaries

In this section, we formalize the framework of LNL, establish the necessary notation, and define the rigorous assumptions that underpin our theoretical analysis.

3.1. Problem Formulation

Let $\mathcal{X} \subseteq \mathbb{R}^d$ be the feature space and $\mathcal{Y} = \{1, \dots, K\}$ be the label space. Let Δ^{K-1} denote the probability simplex

over K classes. We assume the data is generated from a joint distribution \mathcal{D} over $\mathcal{X} \times \mathcal{Y}$. For any instance $x \in \mathcal{X}$, there exists a latent, clean label Y drawn from the conditional posterior $P(Y|X = x)$. However, in the LNL setting, the clean label Y is unobserved. Instead, the learner is presented with a noisy dataset $S_n = \{(x_i, y_i^n)\}_{i=1}^N$, where $y_i^n \in \mathcal{Y}$ represents the observed noisy label.

The label corruption process is governed by an *instance-dependent noise transition matrix* $T : \mathcal{X} \rightarrow [0, 1]^{K \times K}$. The entry $T_{ij}(x)$ represents the probability of the true label i flipping to the noisy label j given the instance x :

$$T_{ij}(x) \triangleq P(Y^n = j | Y = i, X = x). \quad (1)$$

This formulation relates the clean posterior $\eta(x) \triangleq [P(Y = k|x)]_{k=1}^K$ to the noisy posterior $\eta^n(x) \triangleq [P(Y^n = k|x)]_{k=1}^K$ via the linear transformation:

$$\eta^n(x) = T(x)^\top \eta(x). \quad (2)$$

Assumption 3.1 (Diagonal-Dominant Noise). We assume $T(x)$ is diagonally dominant ($T_{ii}(x) > T_{ij}(x), j \neq i$) for all $x \in \mathcal{X}$. Crucially, we *do not* rely on the simplifying assumption of Class-Conditional Noise (CCN); our formulation thus holds for the general, real-world Instance-Dependent Noise (IDN) setting.

3.2. Learning Objectives

The goal is to learn a scoring function $f : \mathcal{X} \rightarrow \mathbb{R}^K$ from a hypothesis class \mathcal{F} . The function $f(x)$ outputs a logit vector, which induces a predicted probability distribution $\hat{p}(x) = \text{softmax}(f(x)) \in \Delta^{K-1}$.

We adopt the *Cross-Entropy (CE) loss* as the base loss function ℓ . The ultimate objective is to minimize the *expected clean risk*:

$$R^c(f) \triangleq \mathbb{E}_{(X,Y) \sim \mathcal{D}}[\ell(f(X), Y)], \quad (3)$$

where $\ell(f(x), y) \triangleq -\log(\hat{p}_y(x))$. Since clean labels are inaccessible, a naive approach is to minimize the *empirical noisy risk* defined on S_n :

$$\hat{R}_{\text{NC}}^n(f) \triangleq \frac{1}{N} \sum_{i=1}^N \ell(f(x_i), y_i^n). \quad (4)$$

We refer to this as the **No Correction (NC)** baseline. Asymptotically, this converges to the expected noisy risk $R_{\text{NC}}^n(f) = \mathbb{E}_{(X,Y^n)}[\ell(f(X), Y^n)]$, which is a biased estimator of $R^c(f)$ and typically yields a suboptimal classifier.

3.3. Risk Correction

To mitigate the bias inherent in $\hat{R}_{\text{NC}}^n(f)$, *statistically consistent* methods construct a surrogate loss function. The gold standard for such methods is achieving *Bayes-classifier*

consistency: $\arg \min_{f \in \mathcal{F}} R_{\text{corr}}^n(f) = \arg \min_{f \in \mathcal{F}} R^c(f)$. While two primary paradigms exist for risk correction—Forward Correction and Backward Correction¹—we focus our analysis on Forward Correction due to its optimization stability and widespread adoption.

Forward Correction (FC). FC explicitly models the noise generation process within the loss function. Instead of correcting the loss gradients (as in BC), FC corrects the model’s prediction. Let $\hat{p}(x)$ be the model’s prediction for the clean class posterior. The predicted probability for the *noisy* class is then given by $T(x)^\top \hat{p}(x)$. The Forward Corrected loss is defined as:

$$\ell_{\text{FC}}(f(x), y^n; x) \triangleq -\log \left([T(x)^\top \hat{p}(x)]_{y^n} \right). \quad (5)$$

Minimizing the expected risk under ℓ_{FC} is proven to be classifier-consistent with the clean risk $R^c(f)$, provided $T(x)$ is known or accurately estimated.

3.4. Evaluation Metrics

To rigorously assess model performance, we employ two complementary metrics:

- **Classification Accuracy (ACC):** Measures the discriminative power of the model with respect to the ground truth labels:

$$\text{ACC}(f) = \mathbb{E}_{(X,Y)} [\mathbb{I}(Y = Y^f(X))],$$

where $Y^f(X) = \arg \max_k \hat{p}_k(X)$.

- **Expected Calibration Error (ECE):** Measures the reliability of the model’s confidence. Let $C^f(X) = \max_k \hat{p}_k(X)$ be the confidence of the prediction. ECE quantifies the expected deviation between confidence and true accuracy:

$$\text{ECE}(f) = \mathbb{E}_C \left[|P(Y = Y^f(X) | C^f(X) = C) - C| \right].$$

4. Theoretical Analysis of Noise Correction

In this section, we dismantle the performance paradox of Forward Risk Correction. A substantial body of literature has established that Forward Correction is *asymptotically consistent* [42, 45]. Formally, let $\mathcal{R}_{\text{FC}}^n(f)$ be the population risk under Forward Correction. It holds that the minimizer $f^* = \arg \min_f \mathcal{R}_{\text{FC}}^n(f)$ coincides with the Bayes-optimal classifier for the clean distribution, i.e., $R^c(f^*) = \min_f R^c(f)$.

¹**Backward Correction (BC)** utilizes the inverse matrix T^{-1} to provide an unbiased risk estimator ($R_{\text{BC}}^n = R^c$). However, we exclude BC from our primary analysis as it suffers from severe numerical instability: T^{-1} typically introduces negative weights, rendering the loss unbounded below and prone to optimization collapse [4, 25].

However, as demonstrated empirically in Figure 1, these theoretical guarantees do not translate to robustness in practice. Even when equipped with the oracle transition matrix $T(x)$, Forward Correction exhibits a characteristic “overfitting” trajectory: accuracy peaks early but degrades significantly during prolonged training, eventually regressing to the performance of the uncorrected baseline (NC).

We posit that this discrepancy is strictly a *finite-sample phenomenon*. Standard asymptotic analysis focuses on the convergence of the population risk $R(f) \rightarrow R^*$. In contrast, deep learning optimization is dominated by the *empirical risk* $\hat{R}(f)$. High-capacity networks are prone to memorizing the finite noisy dataset, driving $\hat{R}(f) \rightarrow \min_f \hat{R}(f)$ even when this empirical minimizer corresponds to a poor population-level solution.

To dissect this failure, our analysis departs from traditional statistical bounds and proceeds in three complementary stages:

1. **Macroscopic Analysis:** We characterize the terminal convergence states, contrasting the ideal population minimizer with the empirical minimizer of the finite noisy dataset.
2. **Microscopic Analysis:** We investigate the optimization dynamics via single-sample gradients to pinpoint the source of memorization.
3. **Fundamental Analysis:** We adopt an information-theoretic perspective to quantify the irreducible information loss induced by the noise channel $T(x)$.

4.1. Theoretical Framework

To evaluate the alignment between the learning objective and the ground truth, we define the following optimal predictors:

- *Clean Bayes-Optimal Classifier* $Y^*(x)$: The most probable class according to the latent clean posterior:

$$Y^*(x) \triangleq \arg \max_{k \in \mathcal{Y}} P(Y = k \mid X = x).$$

- *Inherent Uncertainty* $\delta(x)$: The probability mass assigned to non-optimal classes (aleatoric uncertainty):

$$\delta(x) \triangleq 1 - P(Y = Y^*(x) \mid X = x).$$

Note that unless the clean distribution is deterministic, $\delta(x) > 0$.

- *Noisy Bayes-Optimal Classifier* $\tilde{Y}^*(x)$: The most probable class according to the observed noisy posterior:

$$\tilde{Y}^*(x) \triangleq \arg \max_{k \in \mathcal{Y}} P(Y^n = k \mid X = x).$$

The core difficulty of the LNL problem lies in the misalignment between the clean and noisy objectives. We formalize this by partitioning the input space based on the consistency of these predictors.

Definition 4.1 (Population-Level Consistency Partition). We partition the input space \mathcal{X} into two disjoint sets:

$$\mathcal{X}_{\text{correct}} = \{x \in \mathcal{X} \mid \tilde{Y}^*(x) = Y^*(x)\}$$

$$\mathcal{X}_{\text{error}} = \{x \in \mathcal{X} \mid \tilde{Y}^*(x) \neq Y^*(x)\}$$

Interpretation. $\mathcal{X}_{\text{correct}}$ represents the “benign” regime where the noise, despite corrupting individual samples, preserves the dominant class in the posterior distribution. $\mathcal{X}_{\text{error}}$ represents the “malignant” regime where the noise channel $T(x)$ is sufficiently strong—relative to the clean margin—to flip the optimal decision boundary. Intuitively, samples with high inherent uncertainty $\delta(x)$ (i.e., ambiguous samples close to the decision boundary) are statistically prone to falling into $\mathcal{X}_{\text{error}}$.

Comparison with Prior Art. Most theoretical works before often assume a deterministic clean posterior (i.e., $\delta(x) \equiv 0$). Under this simplification, combined with Assumption 3.1, it strictly holds that $\mathcal{X}_{\text{error}} = \emptyset$. By acknowledging that $\delta(x) \geq 0$, our framework explicitly accounts for the $\mathcal{X}_{\text{error}}$ region and thus generalizes to broader scenarios. As we will show, the behavior of correction methods on this often-overlooked set is crucial.

4.2. Macroscopic Analysis: Ideal vs. Overfitted States

We begin our analysis by examining the two “end states” of the learning process. The central paradox of LNL—its theoretical success (asymptotic consistency) versus its practical failure (overfitting)—is best validated by contrasting these two extremes:

1. **The Ideal Fitted Case** ($R(f) \rightarrow R^*$): This represents the *asymptotic promise* (e.g., $N \rightarrow \infty$). It allows us to establish the theoretical *optimum* of correction methods (i.e., “what we hope to achieve”).
2. **The Empirical Overfitted Case** ($\hat{R}(f) \rightarrow 0$): This represents the *finite-sample reality* of high-capacity deep networks. It models the failure mode where the model memorizes the noisy dataset (i.e., “what we actually observe”).

4.2.1. Analysis of the Ideal Fitted Case

We first analyze the scenario where the optimizer finds the true population minimizer f^* . As established in Section 3.3, Forward Correction (FC) is consistent with the clean distribution, whereas No Correction (NC) targets the noisy distribution. Their optimal population-level predictions $\hat{p}^*(x) = \text{softmax}(f^*(x))$ match the true posteriors:

$$\hat{p}_{\text{NC}}^*(x) = \eta^n(x), \quad \hat{p}_{\text{FC}}^*(x) = \eta(x),$$

where $\eta(x)$ and $\eta^n(x)$ are the clean and noisy posteriors defined in Section 3.1. Based on these posteriors, we charac-

terize their performance using the partition $(\mathcal{X}_{\text{correct}}, \mathcal{X}_{\text{error}})$ from Definition 4.1.

Theorem 4.2 (Optimality and Consistency Gap under Ideal Fitting). *Let f_{NC} and f_{FC} be the ideal population minimizers of the No Correction and Forward Correction risks, respectively.*

(a) **Accuracy (ACC):** *FC achieves the optimal Bayes accuracy. The accuracy gap Δ between FC and NC is non-negative and localized to the error set $\mathcal{X}_{\text{error}}$:*

- $\text{ACC}(f_{\text{FC}}) = 1 - \mathbb{E}_X[\delta(X)]$.
- $\text{ACC}(f_{\text{FC}}) - \text{ACC}(f_{\text{NC}}) = \Delta$.

where

$$\Delta \geq P(\mathcal{X}_{\text{error}}) \cdot \mathbb{E}_{X|\mathcal{X}_{\text{error}}} \left[\max(0, 1 - 2\delta(X)) \right] \geq 0.$$

(b) **Calibration (ECE):** *FC achieves perfect calibration with respect to the clean labels, whereas NC is inherently miscalibrated: $\text{ECE}(f_{\text{FC}}) = 0, \text{ECE}(f_{\text{NC}}) > 0$.*

The proof is provided in Appendix A. Theorem 4.2 provides critical insights that connect our theory to the empirical phenomena observed in Figure 1:

The “Early Peak”. Theorem 4.2 proves FC’s superiority ($\Delta \geq 0$) in the ideal fitted state. This directly explains the “early peak” phenomenon observed in Figure 1. This peak aligns with the well-documented “memorization effect,” where models learn clean, generalizable patterns first. During this initial phase, the network’s state approximates the ideal population minimizer (f_{FC}^*). Since FC is provably superior in this state, it exhibits a clear advantage, successfully correcting the decision boundary before overfitting causes its performance to collapse.

The Role of Inherent Uncertainty. The accuracy gain Δ is structurally tied to the inherent uncertainty $\delta(X)$. As defined, the error set $\mathcal{X}_{\text{error}}$ —where correction is necessary—is predominantly populated by samples with high aleatoric uncertainty (i.e., ambiguous, low-margin samples). This theoretical link directly explains the empirical disparity seen in Figure 1. CIFAR-100, with its more fine-grained classes, possesses higher inherent uncertainty ($\delta(X)$) than CIFAR-10. This implies a larger $\mathcal{X}_{\text{error}}$ region, which, according to our theorem, translates directly to a larger potential accuracy gain (Δ). This perfectly matches the more pronounced improvement FC over NC on CIFAR-100 in the early peak.

4.2.2. Analysis of the Empirical Overfitted Case

We now pivot to the practical failure mode. Modern deep networks typically possess sufficient capacity to drive the empirical risk $\hat{R}(f)$ to its global minimum, a phenomenon widely recognized as *memorization*. To make the analysis of this state tractable, we adopt a simplifying analytical

framework regarding the training data. We consider a hypothetical “full-support, single-label” dataset:

We assume the training set S_n covers the input space \mathcal{X} (full support) and contains exactly one sample pair (x, y^n) for every x , where the noisy label y^n is a single random draw from the conditional distribution $P(Y^n | X = x)$.

The implication of this “full-support” framework is that the global minimization decouples into N independent, per-sample problems. We now analyze the target $\hat{p}(x)$ that minimizes the single-sample loss for (x, y^n) .

• **No Correction (NC):** Minimizing the standard CE loss $\ell_{\text{NC}} = -\log(\hat{p}_{y^n})$ trivially forces the model to memorize the noisy label: $\hat{p}_{\text{NC}}(x) = \mathbf{e}_{y^n}$.

• **Forward Correction (FC):** The objective is to minimize ℓ_{FC} . As we rigorously show in Appendix B, this loss is minimized by collapsing the prediction to a hard vertex corresponding to the largest entry in the y^n -th column of $T(x)$:

$$\hat{p}_{\text{FC}}(x) = \mathbf{e}_{k_{\text{FC}}^*(x)}, \quad (6)$$

where $k_{\text{FC}}^*(x) = \arg \max_k T_{k, y^n}(x)$.

We then formulate the statistical consequences of this collapse in the following theorem. Detailed proofs are provided in Appendix C.

Theorem 4.3 (Accuracy Trade-off and Solution Collapse under Memorization). *Consider the Empirical Overfitted Case where the empirical risk $\hat{R}(f)$ is minimized.*

(a) **Accuracy (ACC):** *In the first-order approximation ($\varepsilon = \mathcal{O}(\mathbb{E}_X[\delta(X)])$), the accuracy of each method is determined by its ability to map the true label Y^* correctly:*

- $\text{ACC}_{\text{NC}} \approx \mathbb{E}_X [(1 - \delta(X))T_{Y^*, Y^*}(X)] + \varepsilon$.
 - $\text{ACC}_{\text{FC}} \approx \mathbb{E}_X [(1 - \delta(X))C_{Y^*}(X)] + \varepsilon$,
- where $C_{Y^*}(X) \triangleq \sum_{j: k^*(j)=Y^*} T_{Y^*, j}(X)$, $k^*(j) = \arg \max_k T_{kj}$.

(d) **Calibration (ECE):** *The prediction confidence collapses to $\hat{c} = 1$ everywhere, resulting in the ECE being perfectly coupled with accuracy: $\text{ECE}_{\text{FC/NC}} = 1 - \text{ACC}_{\text{FC/NC}}$.*

Confirmed Symmetric Collapse. To accurately analyze the accuracy gap $\Delta_{\text{ACC}} \triangleq \text{ACC}_{\text{FC}} - \text{ACC}_{\text{NC}}$ for any general instance-dependent T is analytically intractable across the entire distribution. Though, under symmetric noise, the T -matrix structure ensures $C_{Y^*}(X) = T_{Y^*, Y^*}(X)$. This mathematically proves that the accuracy gap $\Delta_{\text{ACC}} \approx 0$. This confirms the trajectory observed in Figure 1, where the FC and NC performance curves collapse to the same suboptimal level in the prolonged training finally.

Calibration Collapse. The perfect coupling $ECE = 1 - ACC$ suggests that in the overfitted state, the network is not only inaccurate but also *maximally miscalibrated*. The loss function collapses the soft posterior into a deterministic, one-hot vector, providing the theoretical explanation for the extreme overconfidence visible in the experimental ECE plots.

4.3. Microscopic Analysis: The Illusion of Gradient Softening

The remaining challenge in understanding statistical consistency lies in the *transient dynamics* between the ideal asymptotic state ($R \rightarrow R^*$) and the final overfitted state ($\hat{R} \rightarrow 0$). To illuminate this optimization trajectory, we analyze the per-sample gradients.

Let $f_k(\mathbf{x})$ be the logit for class k , inducing the prediction probability $\hat{p}_k = \exp(f_k(\mathbf{x})) / \sum_j \exp(f_j(\mathbf{x}))$. The gradients with respect to the logits $f_k(\mathbf{x})$ are derived as follows:

1. **No Correction (NC) Gradient:** The standard Cross-Entropy loss ℓ_{NC} yields the gradient that pushes the logits directly toward the observed noisy label:

$$\frac{\partial \ell_{\text{NC}}}{\partial f_k(\mathbf{x})} = \hat{p}_k - \mathbb{I}\{y^n = k\}.$$

2. **Forward Correction (FC) Gradient:** The FC loss $\ell_{\text{FC}} = -\log[T(\mathbf{x})^\top \hat{p}(\mathbf{x})]_{y^n}$ yields the corrected gradient (detailed derivation in Appendix D):

$$\frac{\partial \ell_{\text{FC}}}{\partial f_k(\mathbf{x})} = \hat{p}_k - q_k, \quad (7)$$

where $q_k = \frac{T_{k,y^n}(\mathbf{x})\hat{p}_k}{\sum_j T_{j,y^n}(\mathbf{x})\hat{p}_j}$. This term q_k represents the estimated reverse posterior $P(Y = k | Y^n = y^n, \mathbf{x})$.

FC ‘mitigating’ overfitting? We analyze the gradient difference term

$$\Delta_k = \frac{\partial \ell_{\text{NC}}}{\partial f_k} - \frac{\partial \ell_{\text{FC}}}{\partial f_k} = q_k - \mathbb{I}\{y^n = k\}.$$

- **Mitigation:** When $k = y^n$ (the observed label), the FC gradient provides a *weaker push* (less negative magnitude) compared to NC, thereby tempering the tendency to memorize the specific noisy label.
- **Correction:** When $k \neq y^n$, FC allows classes with high likelihood (large $T_{k,y^n}(\mathbf{x})$) to compete for probability mass by *reducing penalties* on alternative classes.

Collectively, FC’s gradient analysis reveals a ‘softening effect’ that guides the model toward the theoretically ideal posterior during intermediate training stages. This mechanism provides the further explanation for the ‘early peak’ observed in Figure 1.

The Inevitable Collapse. The observed softening is, however, an illusion. While the gradients initially encourage a ‘benign’ path, the final convergence behavior² is dictated by the global empirical minimums established in Theorem 4.3. The initial softening of FC is merely the *transient dynamic* of the optimization path as it travels toward its unique, T -biased, and equally pathological hard-vertex attractor $e_{k_{\text{FC}}^*}$.

4.4. Fundamental Analysis: Information Cost of Label Noise

Our analyses in Section 4.2 and Section 4.3 have dissected the specific failure modes of forward correction methods. However, these analyses focus on the properties of the correction *estimators* only. We now step back to consider a more fundamental question: how does the noise process $T(x)$ impact the *data itself*?

This section adopts an information-theoretic perspective to demonstrate that the noise channel $T(x)$ inflicts a *fundamental and universal penalty* by degrading the information content available per sample. This inherent information loss precedes any correction attempt and sets a baseline level of statistical difficulty for *all* LNL strategies.

4.4.1. Quantifying Information in a Single Clean Sample

To quantify the information a label provides about the underlying data-generating process, we adopt a standard setup to quantify the reduction in uncertainty regarding the true process. We consider a finite set of M candidate hypotheses about the true clean posterior, denoted $\{\eta_m(x)\}_{m=1}^M$, drawn from the overall hypothesis space (\mathcal{F}). We assign a prior probability π_m to each hypothesis m . For a fixed input x , the expected posterior under this prior is the mixture $\bar{\eta}(x) \triangleq \sum_{m=1}^M \pi_m \eta_m(x)$.

The information that a single clean label Y at input x reveals about the true underlying hypothesis M is precisely the conditional mutual information $I(M; Y | X = x)$:

$$I_{\text{clean}}(x) \triangleq I(M; Y | X = x)$$

$I_{\text{clean}}(x)$ therefore represents the *maximum statistical signal* available from a clean label at instance x for reducing our uncertainty across the hypothesis space.

4.4.2. Information Contraction via the Noise Channel

In the LNL setting, we observe a noisy label Y^n instead of Y . The generation process follows the Markov chain:

$$M \rightarrow (X, Y) \rightarrow (X, Y^n)$$

The standard Data Processing Inequality (DPI) guarantees that information about M cannot increase along this chain.

²Please refer to Appendix E for a gradient perspective analysis on this.

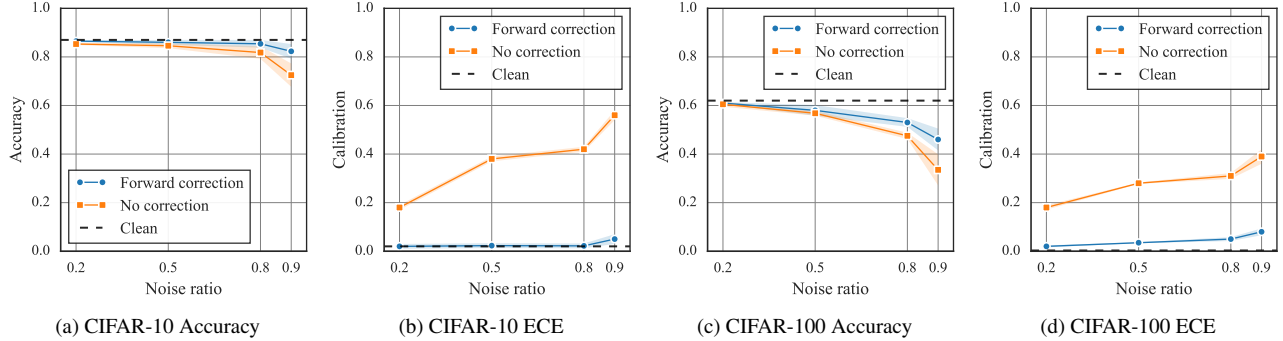


Figure 2. ACC and ECE comparison on CIFAR datasets under Ideal Fitted Case.

Let $q_m(x) = T(x)^\top \eta_m(x)$ be the noisy posterior corresponding to hypothesis m . The conditional information obtainable from a noisy label is:

$$I_{\text{noisy}}(x) \triangleq I(M; Y^n | X = x)$$

Theorem 4.4 (Fundamental Information Cost of Label Noise). *For any fixed input $X = x$, the information content available from the noisy label Y^n is strictly less than or equal to that of the clean label Y :*

$$I_{\text{noisy}}(x) \leq I_{\text{clean}}(x).$$

If the noise channel $T(x)$ is non-trivial (neither Identify nor Permutation), the information contraction is strict, $I_{\text{noisy}}(x) < I_{\text{clean}}(x)$. Detailed proof in Appendix F.

Synthesizing Information Cost and Optimization Failure. This information-theoretic analysis completes our theoretical framework. This *information poverty* provides the final explanation for the LNL paradox. The model overfits not just because the loss function allows it, but because the data itself lacks enough information required to guide the optimization toward the correct, ideal solution $P(Y|X)$.

5. Experiments

This section moves from theoretical diagnosis to empirical validation, structured around three progressive objectives. We first confirm the superior performance of FC in the ideal state. Second, we investigate several methods to promote FC into its optimal generalization state. Finally, motivated by our information-theoretic findings, we conduct scaling experiments to verify the role of per-sample information in mitigating memorization failure. All specific experimental details are provided in Appendix G.

5.1. Validating Ideal State

We first validate the theoretical benefits of noise correction in the Ideal Fitted Case. To *approximate* the ideal functional

form (f^*), we train a linear classifier atop a pretrained encoder, which reduces model complexity while providing robust features.

As shown in Figure 2, the accuracy improvement for FC is clear, particularly at high noise ratios. We attribute this increased accuracy gap to the larger proportion of samples falling into the theoretically derived $\mathcal{X}_{\text{error}}$ region, making boundary correction essential. More importantly, the steady and significant improvement in calibration (ECE), compared to the accuracy gap, directly validates our theory. This confirms that the true benefits of consistency lie in posterior quality, necessitating performance evaluation that extends beyond conventional accuracy metrics.

5.2. An Ideal-State Forcing Framework

Having diagnosed the structural failure of Forward Correction (FC), we now introduce a regularized framework designed to motivate FC into its ideal state. Motivated by literature on model generalization and robust feature learning, we augment noise correction with two lightweight techniques: model pretraining and data interpolation. Specifically, we utilize a self-supervised model pretraining and Mixup augmentations. We consider two modes:

- *FEC (Feature-Enhanced Correction)*: Train a linear classifier on top of a frozen pretrained encoder combined with Mixup and FC.
- *JEC (Joint-Enhanced Correction)*: Jointly train the linear classifier with the pretrained encoder, also combined with Mixup and FC.

We evaluate these two solutions on both CIFAR and the Clothing1M datasets, with results shown in Tab. 1a and Tab. 1b. Historically, noise correction methods have often avoided direct comparison with advanced sample selection methods on mainstream benchmarks. However, we observe that by simply integrating these two lightweight strategies, our new solutions successfully push noise correction toward its ideal state, demonstrating performance that is *fully competitive with* their sample selection counterparts. This confirms the great potential of noise correction methods, ar-

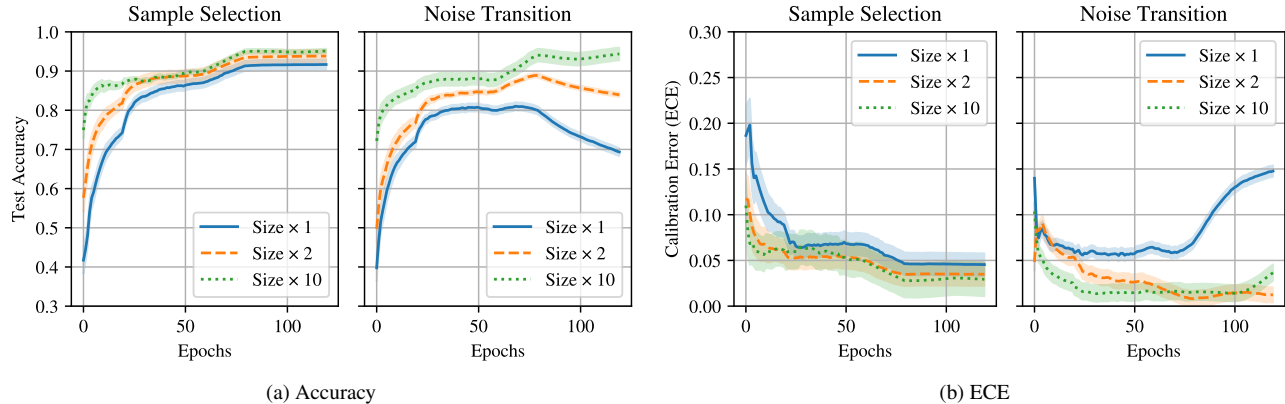


Figure 3. Comparison of Accuracy and ECE for CIFAR-10 on multi-labeled dataset.

Dataset	CIFAR-10					CIFAR-100				Method	Accuracy (%)
	Symmetric				Asymmetric	Symmetric					
	20%	50%	80%	90%	40%	20%	50%	80%	90%		
CE	86.8	79.4	62.9	42.7	85.0	62.0	46.7	19.9	10.1	CE	69.03
Coteaching [62]	89.5	85.7	67.4	47.9	-	65.6	51.8	27.9	13.7	DivideMix [28]	74.76
PENCIL [61]	92.4	89.1	77.5	58.9	88.5	69.4	57.5	31.1	15.3	T-Rev [53]	71.01
LossModel [1]	94.0	92.0	86.8	69.1	87.4	73.9	66.1	48.2	24.3	DualT [60]	71.49
DivideMix [28]	96.1	94.6	93.2	76.0	93.4	77.3	74.6	60.2	31.5	Mixup [64]	71.29
Mixup [64]	95.6	87.1	71.6	52.2	67.8	57.3	30.8	14.6	Forward [45]	69.84	
Forward [45]	86.8	79.8	63.3	42.9	87.2	61.5	46.6	19.9	10.2	FEC (Ours)	61.85
FEC (Ours)	88.1	87.3	85.6	82.5	80.2	60.5	58.6	52.7	44.1	JEC (Ours)	72.24
JEC (Ours)	95.6	88.8	78.5	68.5	93.1	73.1	64.9	50.1	16.2		

(a) Testing accuracy on CIFAR-10 and CIFAR-100 datasets.

(b) Testing accuracy on Clothing1M.

Table 1. Experimental results across datasets.

guing that their empirical failure is not inherent to the approach but rather stems from a lack of effective optimization regularization.

5.3. Noise Correction vs. Sample Selection

In this final section, we assess the fundamental potential of noise correction methods against sample selection techniques. For a fair comparison, we operate under ideal conditions: sample selection is assumed to perfectly identify all clean samples, while noise correction is given the oracle T . This enables us to assess the upper theoretical limit of classification accuracy for both approaches.

To verify the role of data informativeness as suggested in Theorem 4.4, we scale the dataset’s information by scaling from single-label to multi-label samples. Results reported in Figure 3 confirm that as dataset information scales (from 1-label to 10-labels per sample), the ACC of noise correction method steadily improves, approaching that of ideal sample selection. Furthermore, the ECE for noise correction methods is *markedly lower*, underscoring their distinct advantage in retaining predictive confidence.

6. Conclusion

This work rigorously resolves the long-standing paradox about statistically-consistent noise correction methods: their theoretical elegance does not translate into empirical superiority. We prove this failure is not due to estimation error, but rather a structural incompatibility between finite samples and high-capacity optimization. Through a three-pillar analysis, we found that deep networks inevitably collapse into a pathological, T-biased hard vertex. This failure mode is accelerated by a fundamental reduction in sample information caused by the noise channel.

Empirical validation confirmed our findings. We demonstrated that a simple regularization framework successfully promotes Forward Correction (FC) to its ideal generalization state, achieving performance competitive with state-of-the-art sample selection methods. This indicates a paradigm shift in LNL: moving from over-refining the noise matrix T to jointly designing robust losses and optimizers. Beyond label noise, our insights into structural robustness also offer potential benefits for broader applications [9, 14, 16, 17, 40, 41, 49, 57, 58, 63, 69].

Acknowledgements. Georgios Tzimiropoulos’s work was supported by UK Research and Innovation (UKRI) under the UK government’s Horizon Europe funding guarantee (Grant No. 10099264) and by the European Union under Horizon Europe Grant Agreement No. 101135800 (RAIDO).

References

- [1] Eric Arazo, Diego Ortego, Paul Albert, Noel O’Connor, and Kevin McGuinness. Unsupervised label noise modeling and loss correction. In *International Conference on Machine Learning*, pages 312–321. PMLR, 2019. 8
- [2] Shilong Bao, Qianqian Xu, Feiran Li, Boyu Han, Zhiyong Yang, Xiaochun Cao, and Qingming Huang. Towards size-invariant salient object detection: A generic evaluation and optimization approach. *IEEE Transactions on Pattern Analysis and Machine Intelligence*, 2025. 2
- [3] Pengfei Chen, Junjie Ye, Guangyong Chen, Jingwei Zhao, and Pheng-Ann Heng. Beyond class-conditional assumption: A primary attempt to combat instance-dependent label noise. In *Proceedings of the AAAI Conference on Artificial Intelligence*, pages 11442–11450, 2021. 2
- [4] Yu-Ting Chou, Gang Niu, Hsuan-Tien Lin, and Masashi Sugiyama. Unbiased risk estimators can mislead: A case study of learning with complementary labels. In *International conference on machine learning*, pages 1929–1938. PMLR, 2020. 3
- [5] Yuetan Chu, Longxi Zhou, Gongning Luo, Zhaowen Qiu, and Xin Gao. Topology-preserving computed tomography super-resolution based on dual-stream diffusion model. In *International Conference on Medical Image Computing and Computer-Assisted Intervention*, pages 260–270. Springer, 2023. 2
- [6] Yuetan Chu, Gongning Luo, Longxi Zhou, Shaodong Cao, Guolin Ma, Xianglin Meng, Juexiao Zhou, Changchun Yang, Dexuan Xie, Dan Mu, et al. Deep learning-driven pulmonary artery and vein segmentation reveals demography-associated vasculature anatomical differences. *Nature Communications*, 16(1):2262, 2025.
- [7] Yuetan Chu, Yilan Zhang, Zhongyi Han, Changchun Yang, Longxi Zhou, Gongning Luo, Chao Huang, and Xin Gao. Improving representation of high-frequency components for medical visual foundation models. *IEEE Transactions on Medical Imaging*, 44(8):3196–3209, 2025. 2
- [8] Filipe Rolim Cordeiro, Vasileios Belagiannis, Ian Reid, and Gustavo Carneiro. Propmix: Hard sample filtering and proportional mixup for learning with noisy labels. In *32nd British Machine Vision Conference 2021, BMVC 2021, Online, November 22-25, 2021*, page 187. BMVA Press, 2021. 2
- [9] Chen Feng and Ioannis Patras. Adaptive soft contrastive learning. In *2022 26th International Conference on Pattern Recognition (ICPR)*, pages 2721–2727. IEEE, 2022. 2, 8
- [10] Chen Feng and Ioannis Patras. MaskCon: Masked Contrastive Learning for Coarse-Labelled Dataset. In *Proceedings of the IEEE/CVF Conference on Computer Vision and Pattern Recognition (CVPR)*, 2023. 2
- [11] Chen Feng, Georgios Tzimiropoulos, and Ioannis Patras. SSR: An Efficient and Robust Framework for Learning with Unknown Label Noise. In *33rd British Machine Vision Conference (BMVC)*, 2022. 2
- [12] Chen Feng, Georgios Tzimiropoulos, and Ioannis Patras. CLIPCleaner: Cleaning Noisy Labels with CLIP. In *The 32nd ACM International Conference on Multimedia (ACM MM)*, 2024.
- [13] Chen Feng, Georgios Tzimiropoulos, and Ioannis Patras. NoiseBox: Towards More Efficient and Effective Learning with Noisy Labels. *IEEE Transactions on Circuits and Systems for Video Technology*, 2024. 2
- [14] Chen Feng, Ziquan Liu, Zhuo Zhi, Ilija Bogunovic, Carsten Gerner-Beuerle, and Miguel R. D. Rodrigues. PROSAC: Provably safe certification for machine learning models under adversarial attacks. In *The 39th Annual AAAI Conference on Artificial Intelligence (AAAI) [Oral]*, 2025. 8
- [15] Chen Feng, Nicu Sebe, Georgios Tzimiropoulos, Miguel R. D. Rodrigues, and Ioannis Patras. Unveiling open-set noise: Theoretical insights into label noise. In *The 33rd ACM International Conference on Multimedia (ACM MM)*, 2025. 2
- [16] Chen Feng, Minghe Shen, Ananth Balashankar, Carsten Gerner-Beuerle, and Miguel R. D. Rodrigues. Noisy but valid: Robust statistical evaluation of LLMs with imperfect judges. In *The Fourteenth International Conference on Learning Representations (ICLR)*, 2026. 8
- [17] Jiawei Ge, Xinyu Zhang, Jiuxin Cao, Xuelin Zhu, Weijia Liu, Qingqing Gao, Biwei Cao, Kun Wang, Chang Liu, Bo Liu, Chen Feng, and Ioannis Patras. Gen4track: A tuning-free data augmentation framework via self-correcting diffusion model for vision-language tracking. In *Proceedings of the 33rd ACM International Conference on Multimedia*, page 3037–3046, New York, NY, USA, 2025. Association for Computing Machinery. 8
- [18] Aritra Ghosh, Naresh Manwani, and PS Sastry. Making risk minimization tolerant to label noise. *Neurocomputing*, 160: 93–107, 2015. 2
- [19] Jacob Goldberger and Ehud Ben-Reuven. Training deep neural-networks using a noise adaptation layer. In *International conference on learning representations*, 2017. 1
- [20] Bo Han, Quanming Yao, Xingrui Yu, Gang Niu, Miao Xu, Weihua Hu, Ivor Tsang, and Masashi Sugiyama. Co-teaching: Robust training of deep neural networks with extremely noisy labels. *arXiv preprint arXiv:1804.06872*, 2018. 1, 2
- [21] Kaiming He, Xiangyu Zhang, Shaoqing Ren, and Jian Sun. Identity mappings in deep residual networks. In *European conference on computer vision*, pages 630–645. Springer, 2016. 9
- [22] Dan Hendrycks, Mantas Mazeika, Duncan Wilson, and Kevin Gimpel. Using trusted data to train deep networks on labels corrupted by severe noise. *arXiv preprint arXiv:1802.05300*, 2018. 1, 2
- [23] Jiantong Jiang, Peiyu Yang, Rui Zhang, and Feng Liu. Towards efficient large language model serving: A survey on system-aware kv cache optimization. *Authorea Preprints*, 2025. 2

- [24] Nazmul Karim, Mamshad Nayeem Rizve, Nazanin Rahnavard, Ajmal Mian, and Mubarak Shah. Unicon: Combating label noise through uniform selection and contrastive learning. In *Proceedings of the IEEE/CVF Conference on Computer Vision and Pattern Recognition*, pages 9676–9686, 2022. 2
- [25] Ryuichi Kiryo, Gang Niu, Marthinus C Du Plessis, and Masashi Sugiyama. Positive-unlabeled learning with non-negative risk estimator. *Advances in neural information processing systems*, 30, 2017. 3
- [26] Feiran Li, Qianqian Xu, Shilong Bao, Zhiyong Yang, Runmin Cong, Xiaochun Cao, and Qingming Huang. Size-invariance matters: Rethinking metrics and losses for imbalanced multi-object salient object detection. In *International Conference on Machine Learning*, pages 28989–29021. PMLR, 2024. 2
- [27] Feiran Li, Qianqian Xu, Shilong Bao, Boyu Han, Zhiyong Yang, and Qingming Huang. Hybrid generative fusion for efficient and privacy-preserving face recognition dataset generation. In *Proceedings of the IEEE/CVF International Conference on Computer Vision*, pages 495–501, 2025. 2
- [28] Junnan Li, Richard Socher, and Steven CH Hoi. Dividemix: Learning with noisy labels as semi-supervised learning. *arXiv preprint arXiv:2002.07394*, 2020. 1, 2, 8, 10
- [29] Shikun Li, Xiaobo Xia, Shiming Ge, and Tongliang Liu. Selective-supervised contrastive learning with noisy labels. In *Proceedings of the IEEE/CVF Conference on Computer Vision and Pattern Recognition*, pages 316–325, 2022. 1, 2
- [30] Taozhe Li, Guansu Wang, Bo Yu, Yiming Liu, and Wei Sun. Don’t let the information slip away, 2026. 2
- [31] Xuefeng Li, Tongliang Liu, Bo Han, Gang Niu, and Masashi Sugiyama. Provably end-to-end label-noise learning without anchor points. In *International conference on machine learning*, pages 6403–6413. PMLR, 2021. 2
- [32] Junkang Liu, Fanhua Shang, Yuanyuan Liu, Hongying Liu, Yuangang Li, and YunXiang Gong. Fedbcgd: Communication-efficient accelerated block coordinate gradient descent for federated learning. In *Proceedings of the 32nd ACM International Conference on Multimedia*, pages 2955–2963, 2024. 2
- [33] Junkang Liu, Yuanyuan Liu, Fanhua Shang, Hongying Liu, Jin Liu, and Wei Feng. Improving generalization in federated learning with highly heterogeneous data via momentum-based stochastic controlled weight averaging. In *Forty-second International Conference on Machine Learning*, 2025. 2
- [34] Junkang Liu, Fanhua Shang, Yuxuan Tian, Hongying Liu, and Yuanyuan Liu. Consistency of local and global flatness for federated learning. In *Proceedings of the 33rd ACM International Conference on Multimedia*, pages 3875–3883, 2025. 2
- [35] Junkang Liu, Fanhua Shang, Junchao Zhou, Hongying Liu, Yuanyuan Liu, and Jin Liu. Fedmuon: Accelerating federated learning with matrix orthogonalization. *arXiv preprint arXiv:2510.27403*, 2025. 2
- [36] Junkang Liu, Fanhua Shang, Kewen Zhu, Hongying Liu, Yuanyuan Liu, and Jin Liu. Fedadamw: A communication-efficient optimizer with convergence and generalization guarantees for federated large models. *arXiv preprint arXiv:2510.27486*, 2025. 2
- [37] Junkang Liu, Yuxuan Tian, Fanhua Shang, Yuanyuan Liu, Hongying Liu, Junchao Zhou, and Daorui Ding. Dp-fedpgn: Finding global flat minima for differentially private federated learning via penalizing gradient norm. *arXiv preprint arXiv:2510.27504*, 2025. 2
- [38] Tongliang Liu and Dacheng Tao. Classification with noisy labels by importance reweighting. *IEEE Transactions on pattern analysis and machine intelligence*, 38(3):447–461, 2015. 2
- [39] Yang Liu, Hao Cheng, and Kun Zhang. Identifiability of label noise transition matrix. In *International Conference on Machine Learning*, pages 21475–21496. PMLR, 2023. 1, 2
- [40] Haipeng Luo, Qingfeng Sun, Can Xu, Pu Zhao, Qingwei Lin, Jianguang Lou, Shifeng Chen, Yansong Tang, and Weizhu Chen. Arena learning: Build data flywheel for llms post-training via simulated chatbot arena. *arXiv preprint arXiv:2407.10627*, 2024. 8
- [41] Haipeng Luo, Huawen Feng, Qingfeng Sun, Can Xu, Kai Zheng, Yufei Wang, Tao Yang, Han Hu, Yansong Tang, and Di Wang. Agentmath: Empowering mathematical reasoning for large language models via tool-augmented agent. *arXiv preprint arXiv:2512.20745*, 2025. 8
- [42] Nagarajan Natarajan, Inderjit S Dhillon, Pradeep K Ravikumar, and Ambuj Tewari. Learning with noisy labels. *Advances in neural information processing systems*, 26, 2013. 2, 3
- [43] Kento Nishi, Yi Ding, Alex Rich, and Tobias Hollerer. Augmentation strategies for learning with noisy labels. In *Proceedings of the IEEE/CVF Conference on Computer Vision and Pattern Recognition*, pages 8022–8031, 2021. 1
- [44] Diego Ortego, Eric Arazo, Paul Albert, Noel E O’Connor, and Kevin McGuinness. Multi-objective interpolation training for robustness to label noise. In *Proceedings of the IEEE/CVF Conference on Computer Vision and Pattern Recognition*, pages 6606–6615, 2021. 2
- [45] Giorgio Patrini, Alessandro Rozza, Aditya Krishna Menon, Richard Nock, and Lizhen Qu. Making deep neural networks robust to label noise: A loss correction approach. In *Proceedings of the IEEE Conference on Computer Vision and Pattern Recognition*, pages 1944–1952, 2017. 1, 2, 3, 8
- [46] Wentao Qu, Yuantian Shao, Lingwu Meng, Xiaoshui Huang, and Liang Xiao. A conditional denoising diffusion probabilistic model for point cloud upsampling. In *Proceedings of the IEEE/CVF Conference on Computer Vision and Pattern Recognition*, pages 20786–20795, 2024. 2
- [47] Wentao Qu, Jing Wang, Yongshun Gong, Xiaoshui Huang, and Liang Xiao. An end-to-end robust point cloud semantic segmentation network with single-step conditional diffusion models. In *Proceedings of the Computer Vision and Pattern Recognition Conference*, pages 27325–27335, 2025.
- [48] Hwanjun Song, Minseok Kim, and Jae-Gil Lee. Selfie: Refurbishing unclean samples for robust deep learning. In *International Conference on Machine Learning*, pages 5907–5915. PMLR, 2019. 2
- [49] Zhonglin Sun, Chen Feng, Ioannis Patras, and Georgios Tzimiropoulos. LAFS: Landmark-based Facial Self-supervised

- Learning for Face Recognition. In *Proceedings of the IEEE/CVF Conference on Computer Vision and Pattern Recognition (CVPR)*, 2024. 8
- [50] Yisen Wang, Xingjun Ma, Zaiyi Chen, Yuan Luo, Jinfeng Yi, and James Bailey. Symmetric cross entropy for robust learning with noisy labels. In *Proceedings of the IEEE/CVF International Conference on Computer Vision*, pages 322–330, 2019. 2
- [51] Pengxiang Wu, Songzhu Zheng, Mayank Goswami, Dimitris Metaxas, and Chao Chen. A topological filter for learning with label noise. *Advances in neural information processing systems*, 33:21382–21393, 2020. 2
- [52] Zhi-Fan Wu, Tong Wei, Jianwen Jiang, Chaojie Mao, Mingqian Tang, and Yu-Feng Li. Ngc: A unified framework for learning with open-world noisy data. *arXiv preprint arXiv:2108.11035*, 2021. 2
- [53] Xiaobo Xia, Tongliang Liu, Nannan Wang, Bo Han, Chen Gong, Gang Niu, and Masashi Sugiyama. Are anchor points really indispensable in label-noise learning? *Advances in neural information processing systems*, 32, 2019. 1, 2, 8
- [54] Xiaobo Xia, Tongliang Liu, Bo Han, Nannan Wang, Mingming Gong, Haifeng Liu, Gang Niu, Dacheng Tao, and Masashi Sugiyama. Part-dependent label noise: Towards instance-dependent label noise. *Advances in neural information processing systems*, 33:7597–7610, 2020. 2
- [55] Tong Xiao, Tian Xia, Yi Yang, Chang Huang, and Xiaogang Wang. Learning from massive noisy labeled data for image classification. In *Proceedings of the IEEE conference on computer vision and pattern recognition*, pages 2691–2699, 2015. 9
- [56] Mengwei Xie, Shuang Zeng, Xinyuan Chang, Xinran Liu, Zheng Pan, Mu Xu, and Xing Wei. Seqgrowgraph: Learning lane topology as a chain of graph expansions. In *Proceedings of the IEEE/CVF International Conference on Computer Vision*, pages 27166–27175, 2025. 2
- [57] Peiyu Yang, Naveed Akhtar, Zeyi Wen, Mubarak Shah, and Ajmal Saeed Mian. Re-calibrating feature attributions for model interpretation. In *International Conference on Learning Representations*, 2023. 8
- [58] Peiyu Yang, Naveed Akhtar, Jiantong Jiang, and Ajmal Mian. Backdoor-based explainable ai benchmark for high fidelity evaluation of attribution methods. *arXiv preprint arXiv:2405.02344*, 2024. 8
- [59] Peiyu Yang, Naveed Akhtar, Mubarak Shah, and Ajmal Mian. Regulating model reliance on non-robust features by smoothing input marginal density. In *European Conference on Computer Vision*, pages 329–347. Springer, 2024. 2
- [60] Yu Yao, Tongliang Liu, Bo Han, Mingming Gong, Jiankang Deng, Gang Niu, and Masashi Sugiyama. Dual t: Reducing estimation error for transition matrix in label-noise learning. *Advances in neural information processing systems*, 33: 7260–7271, 2020. 1, 2, 8
- [61] Kun Yi and Jianxin Wu. Probabilistic end-to-end noise correction for learning with noisy labels. In *Proceedings of the IEEE/CVF Conference on Computer Vision and Pattern Recognition*, pages 7017–7025, 2019. 8
- [62] Xingrui Yu, Bo Han, Jiangchao Yao, Gang Niu, Ivor Tsang, and Masashi Sugiyama. How does disagreement help generalization against label corruption? In *International Conference on Machine Learning*, pages 7164–7173. PMLR, 2019. 1, 2, 8
- [63] Shuang Zeng, Xinyuan Chang, Mengwei Xie, Xinran Liu, Yifan Bai, Zheng Pan, Mu Xu, and Xing Wei. Futuresight-drive: Thinking visually with spatio-temporal cot for autonomous driving. *arXiv preprint arXiv:2505.17685*, 2025. 8
- [64] Hongyi Zhang, Moustapha Cisse, Yann N Dauphin, and David Lopez-Paz. mixup: Beyond empirical risk minimization. *arXiv preprint arXiv:1710.09412*, 2017. 8
- [65] Rongchao Zhang, Yiwei Lou, Dexuan Xu, Yongzhi Cao, Hanpin Wang, and Yu Huang. A learnable discrete-prior fusion autoencoder with contrastive learning for tabular data synthesis. In *Proceedings of the AAAI Conference on Artificial Intelligence*, pages 16803–16811, 2024. 2
- [66] Rongchao Zhang, Yu Huang, Yongzhi Cao, and Hanpin Wang. Molebridge: Synthetic space projecting with discrete markov bridges. In *The Thirty-ninth Annual Conference on Neural Information Processing Systems*, 2025.
- [67] Rongchao Zhang, Yu Huang, Yiwei Lou, Yi Xin, Haixu Chen, Yongzhi Cao, and Hanpin Wang. Exploit your latents: Coarse-grained protein backmapping with latent diffusion models. In *Proceedings of the AAAI Conference on Artificial Intelligence*, pages 1111–1119, 2025. 2
- [68] Zhilu Zhang and Mert R. Sabuncu. Generalized cross entropy loss for training deep neural networks with noisy labels. *Advances in Neural Information Processing Systems*, 31, 2018. 2
- [69] Zhuo Zhi, Chen Feng, Adam Daneshmend, Mine Orlu, Andreas Demosthenous, Lu Yin, Da Li, Ziquan Liu, and Miguel R. D. Rodrigues. TFAR: A training-free framework for autonomous reliable reasoning in visual question answering. *Transactions on Machine Learning Research*, 2025. 8
- [70] Zhaowei Zhu, Yiwen Song, and Yang Liu. Clusterability as an alternative to anchor points when learning with noisy labels. In *International Conference on Machine Learning*, pages 12912–12923. PMLR, 2021. 2

Deconstructing the Failure of Ideal Noise Correction: A Three-Pillar Diagnosis

Supplementary Material

A. Proofs for the Ideal Fitted Case (Theorem 4.2)

In this appendix, we provide the rigorous derivation for the performance of Forward Correction (FC) and No Correction (NC) in the ideal asymptotic limit ($N \rightarrow \infty$). We rely on the notation defined in the main text: $\eta(x) \triangleq P(Y|X = x)$ denotes the clean posterior, and $\eta^n(x) \triangleq P(Y^n|X = x)$ denotes the noisy posterior. Recall the definition of inherent uncertainty: $\delta(x) \triangleq 1 - \max_k \eta_k(x)$.

A.1. Proof of Theorem 4.2(a): Accuracy Analysis

Proof. We analyze the expected accuracy for both methods and derive the performance gap Δ .

1. Forward Correction (FC). Under the ideal fitted assumption, FC is statistically consistent. It successfully recovers the clean posterior, i.e., $\hat{p}_{\text{FC}}(x) = \eta(x)$. Consequently, the model's prediction $Y_{\text{FC}}^f(x)$ coincides with the Clean Bayes-Optimal classifier $Y^*(x) = \arg \max_k \eta_k(x)$. The accuracy is derived as:

$$\begin{aligned} \text{ACC}(f_{\text{FC}}) &= \mathbb{E}_{(X,Y)} \left[\mathbb{I}(Y = Y_{\text{FC}}^f(X)) \right] \\ &= \mathbb{E}_X \left[\sum_{y \in \mathcal{Y}} P(Y = y|X) \cdot \mathbb{I}(y = Y^*(X)) \right] \\ &= \mathbb{E}_X \left[\eta_{Y^*(X)}(X) \right] \\ &= \mathbb{E}_X [1 - \delta(X)] = 1 - \mathbb{E}_X[\delta(X)]. \end{aligned} \quad (8)$$

This confirms the first claim of Theorem 4.2(a).

2. No Correction (NC). The NC objective minimizes the risk with respect to the noisy labels. The population minimizer yields the noisy posterior $\hat{p}_{\text{NC}}(x) = \eta^n(x)$. Thus, the prediction follows the Noisy Bayes-Optimal classifier $\tilde{Y}^*(x) = \arg \max_k \eta_k^n(x)$. Using the partition from Definition 4.1, we decompose the accuracy via the Law of Total Expectation:

$$\begin{aligned} \text{ACC}(f_{\text{NC}}) &= \mathbb{E}_X \left[P(Y = \tilde{Y}^*(X) | X) \right] \\ &= P(\mathcal{X}_{\text{correct}}) \cdot \mathbb{E}_{X|\mathcal{X}_{\text{correct}}} \left[\eta_{\tilde{Y}^*(X)}(X) \right] + P(\mathcal{X}_{\text{error}}) \cdot \mathbb{E}_{X|\mathcal{X}_{\text{error}}} \left[\eta_{\tilde{Y}^*(X)}(X) \right]. \end{aligned} \quad (9)$$

We analyze the term $\eta_{\tilde{Y}^*(X)}(X)$ in each regime:

- **Regime 1 ($\mathcal{X}_{\text{correct}}$):** By definition, $\tilde{Y}^*(x) = Y^*(x)$. Thus, $\eta_{\tilde{Y}^*(x)}(x) = \eta_{Y^*(x)}(x) = 1 - \delta(x)$.
- **Regime 2 ($\mathcal{X}_{\text{error}}$):** By definition, the predicted class is strictly suboptimal, i.e., $\tilde{Y}^*(x) = k_{\text{err}}$ where $k_{\text{err}} \neq Y^*(x)$.

3. The Accuracy Gap (Δ). The gap is defined as $\Delta \triangleq \text{ACC}(f_{\text{FC}}) - \text{ACC}(f_{\text{NC}})$. Decomposing $\text{ACC}(f_{\text{FC}})$ similarly over the partition, the terms on $\mathcal{X}_{\text{correct}}$ are identical and cancel out. We are left with the difference on the error set:

$$\Delta = P(\mathcal{X}_{\text{error}}) \cdot \mathbb{E}_{X|\mathcal{X}_{\text{error}}} \left[\eta_{Y^*(X)}(X) - \eta_{\tilde{Y}^*(X)}(X) \right]. \quad (10)$$

For any $x \in \mathcal{X}_{\text{error}}$, let $k_{\text{err}} = \tilde{Y}^*(x)$. The probability mass of this erroneous class, $\eta_{k_{\text{err}}}(x)$, is bounded by two constraints:

1. It is sub-optimal: $\eta_{k_{\text{err}}}(x) \leq \eta_{Y^*(x)}(x) = 1 - \delta(x)$.
2. It is part of the residual mass: $\eta_{k_{\text{err}}}(x) \leq \sum_{k \neq Y^*} \eta_k(x) = \delta(x)$.

Thus, $\eta_{k_{\text{err}}}(x) \leq \min(\delta(x), 1 - \delta(x))$. Substituting this into the gap equation:

$$\begin{aligned} \eta_{Y^*(x)}(x) - \eta_{k_{\text{err}}}(x) &\geq (1 - \delta(x)) - \min(\delta(x), 1 - \delta(x)) \\ &= \max(0, 1 - 2\delta(x)). \end{aligned} \quad (11)$$

Therefore, the lower bound for the gap is:

$$\Delta \geq P(\mathcal{X}_{\text{error}}) \cdot \mathbb{E}_{X|\mathcal{X}_{\text{error}}} \left[\max(0, 1 - 2\delta(X)) \right] \geq 0. \quad (12)$$

This proves the non-negative gap and completes the proof for Part (a). \square

A.2. Proof of Theorem 4.2(b): ECE Analysis

Proof. Let $C(X) = \max_k \hat{p}_k(X)$ be the prediction confidence and $Y^f(X) = \arg \max_k \hat{p}_k(X)$ be the predicted label. The Expected Calibration Error (ECE) is defined as:

$$\text{ECE}(f) = \mathbb{E}_C \left[|P(Y = Y^f(X) | C(X) = C) - C| \right]. \quad (13)$$

By defining the *per-sample calibration gap* as $\Delta_{\text{cal}}(x) \triangleq |P(Y = Y^f(x)|x) - \hat{p}_{Y^f(x)}(x)|$, we can rewrite the ECE as the expected local calibration error:

$$\text{ECE}(f) = \mathbb{E}_X [\Delta_{\text{cal}}(X)]. \quad (14)$$

1. Forward Correction (FC). In the ideal case, $\hat{p}_{\text{FC}}(x) = \eta(x)$. The confidence is $C(x) = \eta_{Y^*(x)}(x)$. The true accuracy of this prediction is $P(Y = Y^*(x)|x) = \eta_{Y^*(x)}(x)$. Since the model output matches the ground truth posterior, the gap vanishes:

$$\Delta_{\text{cal}}^{\text{FC}}(x) = |\eta_{Y^*(x)}(x) - \eta_{Y^*(x)}(x)| = 0 \implies \text{ECE}(f_{\text{FC}}) = 0. \quad (15)$$

2. No Correction (NC). In the ideal case, $\hat{p}_{\text{NC}}(x) = \eta^n(x)$. The model's confidence is derived from the noisy posterior: $C(x) = \eta_{\hat{Y}^*(x)}^n(x)$. However, the true correctness of the prediction depends on the clean posterior: $P(Y = \hat{Y}^*(x)|x) = \eta_{\hat{Y}^*(x)}(x)$. The calibration gap is:

$$\Delta_{\text{cal}}^{\text{NC}}(x) = \left| \eta_{\hat{Y}^*(x)}(x) - \eta_{\hat{Y}^*(x)}^n(x) \right|. \quad (16)$$

Unless the transition matrix $T(x)$ is the identity (no noise) or a specific permutation that preserves diagonal dominance exactly, generally $\eta(x) \neq \eta^n(x)$. Thus, $\Delta_{\text{cal}}^{\text{NC}}(x) > 0$ for some x , implying $\text{ECE}(f_{\text{NC}}) > 0$. \square

B. Derivation of the Empirical Minimizer for FC (Eq. 6)

In this section, we provide the formal derivation for the optimal solution $\hat{p}(x)$ that minimizes the single-sample Forward Correction (FC) loss.

1. Optimization Problem. We analyze the failure mode where a high-capacity network memorizes the training set, driving the empirical risk $\hat{R}(f) \rightarrow 0$. This implies minimizing the loss for each sample (x, y^n) independently.

The single-sample FC loss for a prediction $\hat{p}(x)$ is:

$$\ell_{\text{FC}}(\hat{p}(x) | x, y^n) = -\log \left(\sum_{k=1}^K T_{k, y^n}(x) \cdot \hat{p}_k(x) \right). \quad (17)$$

Our objective is to find the optimal probability vector \hat{p}^* that minimizes this loss, subject to the constraint that \hat{p}^* lies on the probability simplex Δ^{K-1} :

$$\hat{p}^* = \arg \min_{\hat{p} \in \Delta^{K-1}} \ell_{\text{FC}}(\hat{p} | x, y^n). \quad (18)$$

2. Equivalent Linear Objective. The function $g(z) = -\log(z)$ is strictly monotonically decreasing for $z > 0$. Therefore, minimizing ℓ_{FC} is mathematically equivalent to maximizing its argument:

$$\hat{p}^* = \arg \max_{\hat{p} \in \Delta^{K-1}} \left(\sum_{k=1}^K T_{k, y^n}(x) \cdot \hat{p}_k \right). \quad (19)$$

3. Solution via Linear Programming. For a fixed sample (x, y^n) , the transition probabilities $T_{k,y^n}(x)$ (which form the y^n -th column of $T(x)$) are constants. Let us define a constant vector $\mathbf{c} \in \mathbb{R}^K$ where each element $c_k = T_{k,y^n}(x)$.

The optimization problem simplifies to:

$$\arg \max_{\hat{p} \in \Delta^{K-1}} (\mathbf{c}^\top \hat{p}). \quad (20)$$

This is a **Linear Program (LP)**: we are maximizing a linear objective function $(\mathbf{c}^\top \hat{p})$ over a convex polytope (the probability simplex Δ^{K-1}).

4. Optimal Solution at Vertex. A fundamental theorem of linear programming states that the maximum of a linear function over a convex polytope must be achieved at one of the polytope’s vertices. The vertices of the probability simplex Δ^{K-1} are the set of standard basis vectors (one-hot vectors):

$$\mathcal{V} = \{\mathbf{e}_1, \mathbf{e}_2, \dots, \mathbf{e}_K\}.$$

To find the optimal solution, we evaluate the objective function at each vertex \mathbf{e}_j :

$$\mathbf{c}^\top \mathbf{e}_j = \sum_{k=1}^K c_k \cdot (\mathbf{e}_j)_k = c_j = T_{j,y^n}(x).$$

The objective is maximized by choosing the vertex \mathbf{e}_{k^*} that corresponds to the largest coefficient c_{k^*} . We define this optimal index k^* as:

$$k_{\text{FC}}^*(x) \triangleq \arg \max_{k \in \{1, \dots, K\}} T_{k,y^n}(x).$$

Therefore, the unique optimal solution that minimizes the single-sample FC loss is:

$$\hat{p}^* = \mathbf{e}_{k_{\text{FC}}^*(x)}.$$

This completes the derivation of Equation (6).

Implications. This derivation formally proves that the empirical minimizer of the FC loss is *not* the “correct” soft posterior $\eta(x)$. Instead, the loss function creates an optimization landscape whose global minimum (for a finite sample) is a hard, one-hot vector.

C. Proofs for the Empirical Overfitted Case (Theorem 4.3)

In this appendix, we provide the detailed derivations for the accuracy and calibration properties in the “Empirical Overfitted Case” (Section 4.2.2). We assume the model has memorized the training data, collapsing its predictions to one-hot vectors as derived in Section B.

We use the notation $\eta_k(x) \triangleq P(Y = k \mid X = x)$ for the clean posterior and $\delta(x) \triangleq 1 - \eta_{Y^*}(x)$ for the inherent uncertainty. The accuracy is $\text{ACC} = \mathbb{E}_X[P(Y^f = Y \mid X)]$.

C.1. Proof of Theorem 4.3(a): Accuracy (ACC)

We first derive the exact conditional accuracy $\text{ACC}(x) = P(Y^f = Y \mid X = x)$ for both methods.

No Correction (NC) The NC solution memorizes the noisy label, so $Y^f = Y^n$. The conditional accuracy is the probability that the observed noisy label matches the (unseen) true clean label.

$$\begin{aligned}
\text{ACC}_{\text{NC}}(x) &= P(Y^f = Y \mid x) = P(Y^n = Y \mid x) \\
&= \sum_{k \in \mathcal{Y}} P(Y^n = Y, Y = k \mid x) \\
&= \sum_{k \in \mathcal{Y}} P(Y^n = k, Y = k \mid x) \quad (\text{since } Y^n = Y \text{ implies } Y^n = k \text{ and } Y = k) \\
&= \sum_{k=1}^K P(Y^n = k \mid Y = k, x) P(Y = k \mid x) \\
&= \sum_{k=1}^K T_{k,k}(x) \eta_k(x)
\end{aligned} \tag{21}$$

To analyze its dependence on $\delta(x)$, we split the sum into the dominant class ($k = Y^*$) and the residual $\mathcal{R}_{\text{NC}}(x)$:

$$\begin{aligned}
\text{ACC}_{\text{NC}}(x) &= \eta_{Y^*}(x) T_{Y^*, Y^*}(x) + \sum_{k \neq Y^*} \eta_k(x) T_{k,k}(x) \\
&= (1 - \delta(x)) T_{Y^*, Y^*}(x) + \mathcal{R}_{\text{NC}}(x)
\end{aligned} \tag{22}$$

Since $0 \leq T_{k,k}(x) \leq 1$ and $\sum_{k \neq Y^*} \eta_k(x) = \delta(x)$, the residual is bounded: $0 \leq \mathcal{R}_{\text{NC}}(x) \leq \delta(x)$. Thus, $\mathcal{R}_{\text{NC}}(x) = \mathcal{O}(\delta(x))$. The dominant first-order approximation is:

$$\text{ACC}_{\text{NC}}(x) \approx (1 - \delta(x)) T_{Y^*, Y^*}(x) \tag{23}$$

Forward Correction (FC) From Section B, the FC prediction is $Y^f = k^*(Y^n)$, where $k^*(j) \triangleq \arg \max_k T_{k,j}(x)$. The conditional accuracy is the probability that this prediction matches the true label Y .

$$\begin{aligned}
\text{ACC}_{\text{FC}}(x) &= P(Y^f = Y \mid x) = P(k^*(Y^n) = Y \mid x) \\
&= \sum_{k \in \mathcal{Y}} P(k^*(Y^n) = Y, Y = k \mid x) \\
&= \sum_{k \in \mathcal{Y}} P(Y = k \mid x) P(k^*(Y^n) = k \mid Y = k, x) \quad (\text{as } Y^n \text{ depends on } Y) \\
&= \sum_{k=1}^K \eta_k(x) \left(\sum_{j: k^*(j)=k} P(Y^n = j \mid Y = k, x) \right) \\
&= \sum_{k=1}^K \eta_k(x) \underbrace{\left(\sum_{j: k^*(j)=k} T_{k,j}(x) \right)}_{\triangleq C_k(x)}
\end{aligned} \tag{24}$$

Let $C_k(x)$ be the sum of probabilities of transitions from class k to any noisy label j that maps back to k . The exact accuracy is $\text{ACC}_{\text{FC}}(x) = \sum_k \eta_k(x) C_k(x)$. We split this sum:

$$\begin{aligned}
\text{ACC}_{\text{FC}}(x) &= \eta_{Y^*}(x) C_{Y^*}(x) + \sum_{k \neq Y^*} \eta_k(x) C_k(x) \\
&= (1 - \delta(x)) C_{Y^*}(x) + \mathcal{R}_{\text{FC}}(x)
\end{aligned} \tag{25}$$

Since $C_k(x) = \sum_{j: \dots} T_{k,j}(x) \leq \sum_j T_{k,j}(x) = 1$, the residual $\mathcal{R}_{\text{FC}}(x)$ is also $\mathcal{O}(\delta(x))$. The first-order approximation is:

$$\text{ACC}_{\text{FC}}(x) \approx (1 - \delta(x)) C_{Y^*}(x) \tag{26}$$

Comparison: The Gain/Loss Trade-off The relative performance is driven by the difference between $C_{Y^*}(x)$ and $T_{Y^*,Y^*}(x)$. The first-order accuracy gap is:

$$\Delta_{\text{ACC}}(x) \approx (1 - \delta(x)) [C_{Y^*}(x) - T_{Y^*,Y^*}(x)] \quad (27)$$

To understand this gap, we decompose $C_{Y^*}(x)$ by splitting its sum at $j = Y^*$:

$$\begin{aligned} C_{Y^*}(x) &= \sum_{j:k^*(j)=Y^*} T_{Y^*,j}(x) \\ &= T_{Y^*,Y^*}(x) \cdot \mathbb{I}(k^*(Y^*) = Y^*) + \sum_{j \neq Y^*} T_{Y^*,j}(x) \cdot \mathbb{I}(k^*(j) = Y^*) \end{aligned} \quad (28)$$

Substituting this into the gap equation $[C_{Y^*}(x) - T_{Y^*,Y^*}(x)]$ yields:

$$\begin{aligned} &= \left[T_{Y^*,Y^*}(x) \mathbb{I}(k^*(Y^*) = Y^*) + \sum_{j \neq Y^*} \dots \right] - T_{Y^*,Y^*}(x) \\ &= \sum_{j \neq Y^*} T_{Y^*,j}(x) \mathbb{I}(k^*(j) = Y^*) + T_{Y^*,Y^*}(x) (\mathbb{I}(k^*(Y^*) = Y^*) - 1) \\ &= \underbrace{\sum_{j \neq Y^*} T_{Y^*,j}(x) \mathbb{I}(k^*(j) = Y^*)}_{\text{Gain: Errors corrected by FC}} - \underbrace{T_{Y^*,Y^*}(x) \mathbb{I}(k^*(Y^*) \neq Y^*)}_{\text{Loss: Correct labels mis-corrected by FC}} \end{aligned} \quad (29)$$

This confirms that FC’s performance is a fragile trade-off: it gains accuracy only if it correctly maps erroneous labels (like $j \neq Y^*$) back to Y^* , but it loses accuracy if it maps the *correct* label Y^* to something else ($k^*(Y^*) \neq Y^*$).

Intuition and Visualization of the Gain/Loss Trade-off. To build a strong intuition for the trade-off just derived in Equation (29), we provide a concrete visualization of the collapsed solution $k^*(j) \triangleq \arg \max_k T_{k,j}(x)$. This is a deterministic lookup table found by scanning each **column** j of the T -matrix to find the **row** k with the maximum value.

Consider this 3-class “pathological” but valid T-matrix (rows sum to 1, column max bolded):

$$T(x) = \begin{matrix} & Y^n = \text{Bird (j=1)} & Y^n = \text{Dog (j=2)} & Y^n = \text{Cat (j=3)} \\ \begin{matrix} Y = \text{Bird (k=1)} \\ Y = \text{Dog (k=2)} \\ Y = \text{Cat (k=3)} \end{matrix} & \begin{pmatrix} \mathbf{0.5} & \mathbf{0.45} & 0.05 \\ 0.25 & \mathbf{0.4} & \mathbf{0.35} \\ 0.33 & 0.33 & 0.34 \end{pmatrix} \end{matrix}$$

The lookup table $k^*(j)$ becomes (based on the column-wise bolded maximums):

- $k^*(1) = \arg \max(0.5, 0.25, 0.33) = 1$ (Observed ‘Bird’ → Predict ‘Bird’)
- $k^*(2) = \arg \max(0.45, 0.4, 0.33) = 1$ (Observed ‘Dog’ → Predict ‘Bird’)
- $k^*(3) = \arg \max(0.05, 0.35, 0.34) = 2$ (Observed ‘Cat’ → Predict ‘Dog’)

This pathological mapping $j \rightarrow k^*(j)$ directly explains the Gain/Loss terms from Equation (29):

- **Loss Term Activation** ($\mathbb{I}(k^*(Y^*) \neq Y^*)$): This term activates when a “correct” noisy label is “mis-corrected”. For example, if the true label is $Y^* = 2$ (‘Dog’) and the noisy label is also $Y^n = 2$ (a correct pair), the NC baseline would be correct. However, the FC model uses its lookup table, finds $k^*(2) = 1$, and predicts ‘Bird’, thus **creating a loss**. The same occurs for $Y^* = 3$ (‘Cat’), where the correct label $Y^n = 3$ is mapped to $k^*(3) = 2$.
- **Gain Term Activation** ($\mathbb{I}(k^*(j) = Y^*)$ for $j \neq Y^*$): This term activates when an “incorrect” noisy label is “corrected”. For example, if the true label is $Y^* = 1$ (‘Bird’) but the noisy label is $Y^n = 2$ (‘Dog’) (an error pair), the NC baseline would be wrong. However, the FC model finds $k^*(2) = 1$, which matches $Y^* = 1$, thus **creating a gain**. The same occurs for $Y^* = 2$ (‘Dog’) when $Y^n = 3$ (‘Cat’), as $k^*(3) = 2$.

Therefore, the performance of the overfitted FC model depends on the fragile balance between these gain and loss terms, which are dictated entirely by the T-matrix structure.

Symmetric Noise Case. Now we apply this framework to the symmetric noise case. With rate $\rho < (K - 1)/K$, the T-matrix is constant, and $T_{j,j} = 1 - \rho > T_{i,j} = \rho/(K - 1)$ for $i \neq j$. This means the maximum of every column j is strictly on the diagonal. Therefore:

$$k^*(j) = j \quad \text{for all } j.$$

We plug this into the Gain/Loss equation (Equation (29)):

- **Gain Term:** $\sum_{j \neq Y^*} T_{Y^*,j} \mathbb{I}(j = Y^*) = 0$ (the sum is over an empty set).
- **Loss Term:** $T_{Y^*,Y^*} \mathbb{I}(Y^* \neq Y^*) = 0$.

The first-order accuracy gap is zero: $\text{ACC}_{\text{FC}}(x) \approx \text{ACC}_{\text{NC}}(x)$. The total accuracy for both methods collapses to:

$$\text{ACC} \approx \mathbb{E}_X [(1 - \delta(x))(1 - \rho)] = (1 - \rho)(1 - \mathbb{E}[\delta(X)])$$

This analytically confirms the ‘‘solution collapse’’ to the same suboptimal baseline observed in Figure 1.

C.2. Proof of Theorem 4.3(b): ECE

Proof. For both NC and FC, the overfitted solution is a one-hot vector (e.g., $\hat{p} = \mathbf{e}_{k^*}$). The prediction confidence is therefore $C(X) = \max_k \hat{p}_k(X) = 1$ for all samples. The ECE formula is defined as $\text{ECE}(f) = \mathbb{E}_C [|P(Y = Y^f | C) - C|]$. Since $C = 1$ everywhere, the expectation simplifies to a single point:

$$\begin{aligned} \text{ECE}(f) &= |P(Y = Y^f | C = 1) - 1| \\ &= |P(Y = Y^f) - 1| \quad (\text{since } C = 1 \text{ provides no new information}) \\ &= |\text{ACC}(f) - 1| \\ &= 1 - \text{ACC}(f) \quad (\text{since } \text{ACC}(f) \leq 1) \end{aligned} \tag{30}$$

This proves that in the overfitted, hard-label regime, ECE is perfectly and negatively coupled with accuracy. \square

D. Gradient Derivation for Forward Correction (FC)

In this section, we derive the gradient of the Forward Corrected loss ℓ_{FC} with respect to a single logit $f_k(x)$, as referenced in Section 4.3.

The loss for a single sample (x, y^n) is defined as:

$$\ell_{\text{FC}} = -\log(z_{y^n}) \tag{31}$$

where z is the model’s predicted noisy posterior vector, $z = T(x)^\top \hat{p}(x)$, and $\hat{p}(x) = \text{softmax}(f(x))$. The term z_{y^n} is the single component corresponding to the observed noisy label y^n :

$$z_{y^n} = \sum_{i=1}^K T_{i,y^n}(x) \hat{p}_i(x)$$

We use the chain rule to compute $\frac{\partial \ell_{\text{FC}}}{\partial f_k}$:

$$\frac{\partial \ell_{\text{FC}}}{\partial f_k} = \frac{\partial \ell_{\text{FC}}}{\partial z_{y^n}} \cdot \frac{\partial z_{y^n}}{\partial f_k}$$

Step 1: Derivative of Loss w.r.t. z_{y^n} The derivative of the negative logarithm is:

$$\frac{\partial \ell_{\text{FC}}}{\partial z_{y^n}} = -\frac{1}{z_{y^n}}$$

Step 2: Derivative of z_{y^n} w.r.t. logit f_k We apply the chain rule again, summing over all clean probabilities \hat{p}_j :

$$\begin{aligned} \frac{\partial z_{y^n}}{\partial f_k} &= \sum_{j=1}^K \frac{\partial z_{y^n}}{\partial \hat{p}_j} \cdot \frac{\partial \hat{p}_j}{\partial f_k} \\ &= \sum_{j=1}^K T_{j,y^n}(x) \cdot \frac{\partial \hat{p}_j}{\partial f_k} \end{aligned}$$

We use the standard softmax derivative $\frac{\partial \hat{p}_j}{\partial f_k} = \hat{p}_j(\delta_{jk} - \hat{p}_k)$, where δ_{jk} is the Kronecker delta.

$$\begin{aligned}
\frac{\partial z_{y^n}}{\partial f_k} &= \sum_{j=1}^K T_{j,y^n} \hat{p}_j (\delta_{jk} - \hat{p}_k) \\
&= \underbrace{T_{k,y^n} \hat{p}_k (1 - \hat{p}_k)}_{\text{Case } j=k} + \underbrace{\sum_{j \neq k} T_{j,y^n} \hat{p}_j (-\hat{p}_k)}_{\text{Case } j \neq k} \\
&= (T_{k,y^n} \hat{p}_k - T_{k,y^n} \hat{p}_k^2) - \hat{p}_k \sum_{j \neq k} T_{j,y^n} \hat{p}_j \\
&= T_{k,y^n} \hat{p}_k - \hat{p}_k \left(T_{k,y^n} \hat{p}_k + \sum_{j \neq k} T_{j,y^n} \hat{p}_j \right) \\
&= T_{k,y^n} \hat{p}_k - \hat{p}_k \left(\sum_{j=1}^K T_{j,y^n} \hat{p}_j \right) \\
&= T_{k,y^n} \hat{p}_k - \hat{p}_k z_{y^n}
\end{aligned}$$

Step 3: Combining the Terms We substitute the results from Step 1 and Step 2 back into the main chain rule formula:

$$\begin{aligned}
\frac{\partial \ell_{\text{FC}}}{\partial f_k} &= \left(-\frac{1}{z_{y^n}} \right) \cdot (T_{k,y^n} \hat{p}_k - \hat{p}_k z_{y^n}) \\
&= -\frac{T_{k,y^n} \hat{p}_k}{z_{y^n}} + \frac{\hat{p}_k z_{y^n}}{z_{y^n}} \\
&= \hat{p}_k - \frac{T_{k,y^n} \hat{p}_k}{z_{y^n}}
\end{aligned} \tag{32}$$

Recalling the definition $z_{y^n} = \sum_j T_{j,y^n} \hat{p}_j$, we obtain the final form presented in Equation (7):

$$\frac{\partial \ell_{\text{FC}}}{\partial f_k(x)} = \hat{p}_k - q_k \tag{33}$$

where $q_k = \frac{T_{k,y^n}(x) \hat{p}_k}{\sum_j T_{j,y^n}(x) \hat{p}_j}$. As noted in the main text, this q_k term is precisely the model’s estimated reverse posterior $P(Y = k | Y^n = y^n, x)$ via Bayes’ rule.

This gradient form $\hat{p}_k - q_k$ should be contrasted with the standard Cross-Entropy gradient, $\hat{p}_k - \mathbb{I}\{y^n = k\}$. Instead of a hard ‘1’ pulling the gradient for the observed class, FC uses a ‘soft’ target q_k distributed over all classes k , which explains the ‘gradient softening’ effect discussed in the main paper.

E. Analysis of Optimization Dynamics and Gradient Saturation

In this appendix, we analyze the optimization dynamics of the Forward Correction (FC) loss. As shown in Appendix B, the theoretical global minimum of the single-sample (overfitted) loss is not the clean label \mathbf{e}_{y^*} , but the ‘collapsed’ solution $\mathbf{e}_{k_{\text{FC}}^*}$. Here, we show here that the practical optimization path does not even guarantee convergence to this theoretical minimum.

Our analysis proceeds in two steps:

1. **Global Gradient Flow:** We first analyze the vector field of the gradient $\nabla_{\mathbf{f}} \ell_{\text{FC}}$. We confirm that the gradient flow, when viewed globally, does indeed point towards the correct theoretical minimum $\mathbf{e}_{k_{\text{FC}}^*}$ (the solution from the Linear Program analysis in Appendix B).
2. **Local Gradient Saturation:** We then show that due to the Softmax parameterization, the gradient magnitude vanishes near *all* simplex vertices. This creates ‘dead zones’ (local minima) around sub-optimal attractors, most notably the noisy label vertex \mathbf{e}_{y^n} .

This analysis demonstrates that while the loss function’s *global* landscape points to $\mathbf{e}_{k_{\text{FC}}^*}$, its *local* properties trap the optimizer. The final ‘pseudo-converged’ solution is therefore path-dependent, not guaranteed to be the theoretical optimum, and often defaults to the noisy vertex \mathbf{e}_{y^n} due to early-learning dynamics.

Theoretical Optimum and Global Gradient Flow As derived in Appendix B, the FC loss for a sample (x, y^n) is:

$$\ell_{\text{FC}}(\hat{\mathbf{p}}) = -\log \left(\sum_{k=1}^K \hat{p}_k T_{k, y^n} \right) \quad (34)$$

Minimizing this is equivalent to the Linear Program $\max_{\hat{\mathbf{p}} \in \Delta^{K-1}} \sum_{k=1}^K \hat{p}_k T_{k, y^n}$. The global optimum $\hat{\mathbf{p}}^*$ is the one-hot vector $\mathbf{e}_{k_{\text{FC}}^*}$, where $k_{\text{FC}}^* = \arg \max_k T_{k, y^n}$.

An analysis of the gradient flow (as visualized on a 3-class simplex example in Fig. 4) confirms this. The vector field of the gradient $\nabla_{\mathbf{f}} \ell_{\text{FC}}$ globally points away from all other vertices and towards the single vertex $\mathbf{e}_{k_{\text{FC}}^*}$. Theoretically, a gradient descent algorithm with perfect information should converge to k_{FC}^* .

Gradient Saturation and Pseudo-Convergence The practical failure arises from the Softmax parameterization $\hat{p}_k = \text{softmax}(f_k)$. The gradient of the loss with respect to the logits \mathbf{f} is:

$$\frac{\partial \ell}{\partial f_k} = \sum_{j=1}^K \frac{\partial \ell}{\partial \hat{p}_j} \frac{\partial \hat{p}_j}{\partial f_k} \quad (35)$$

The Softmax derivative $\frac{\partial \hat{p}_j}{\partial f_k} = \hat{p}_j (\delta_{jk} - \hat{p}_k)$ approaches 0 as $\hat{\mathbf{p}}$ approaches *any* vertex \mathbf{e}_i . Consequently, the magnitude of the logit gradient vanishes near all vertices:

$$\lim_{\hat{\mathbf{p}} \rightarrow \mathbf{e}_i} \|\nabla_{\mathbf{f}} \ell_{\text{FC}}\| \approx 0 \quad \text{for any } i \in \{1, \dots, K\} \quad (36)$$

This phenomenon creates “gradient plateaus” or “dead zones” around *every* vertex.

Dynamics Analysis: Trapped in a Local Minimum The existence of these “dead zones” means the final convergence point is path-dependent. In Noisy Label Learning, models famously exhibit an “early learning” phase (fitting simple patterns) followed by a “memorization” phase (fitting noisy labels).

1. The model quickly learns to fit the dominant noisy labels, causing its prediction $\hat{\mathbf{p}}$ to approach the noisy vertex \mathbf{e}_{y^n} .
2. As $\hat{\mathbf{p}} \rightarrow \mathbf{e}_{y^n}$, the model enters the gradient saturation “dead zone” of this vertex.
3. Although \mathbf{e}_{y^n} is not the global minimum of ℓ_{FC} (assuming $k_{\text{FC}}^* \neq y^n$), the gradient pointing away from \mathbf{e}_{y^n} and towards the true minimum $\mathbf{e}_{k_{\text{FC}}^*}$ becomes infinitesimally small.
4. SGD, with limited step size, fails to escape this local basin of attraction.

This results in *pseudo-convergence*: the model remains “trapped” at the wrong label \mathbf{e}_{y^n} . Therefore, the actual overfitted solution observed in practice is not the theoretical optimum $\mathbf{e}_{k_{\text{FC}}^*}$, but rather a sub-optimal local minimum \mathbf{e}_{y^n} that acts as a strong attractor.

F. Proof of Theorem 4.4: Fundamental Information Cost

We provide the rigorous proof for Theorem 4.4. We restate the definitions for a fixed input $X = x$:

- $I_{\text{clean}}(x) \triangleq I(M; Y \mid X = x)$
- $I_{\text{noisy}}(x) \triangleq I(M; Y^n \mid X = x)$

Our goal is to prove that $I_{\text{noisy}}(x) \leq I_{\text{clean}}(x)$.

1. Establishing the Conditional Markov Chain The data-generating process described in Section 4.4 forms a conditional Markov chain for any fixed $X = x$:

$$M \rightarrow Y \rightarrow Y^n \quad \text{conditioned on } X = x.$$

This holds because:

1. The hypothesis M (which represents the true data-generating process $\eta_m(x)$) determines the distribution for the clean label Y .
2. The noisy label Y^n is generated based *only* on the clean label Y (via the noise channel $T(x)$), without any direct influence from M .

Therefore, given Y , the noisy label Y^n is conditionally independent of the hypothesis M . This conditional independence implies:

$$I(M; Y^n \mid Y, X = x) = 0. \quad (37)$$

2. Applying the Chain Rule for Mutual Information We decompose the joint mutual information $I(M; Y, Y^n | X = x)$ in two different ways using the chain rule:

- **Decomposition 1 (Grouping with Y):**

$$\begin{aligned} I(M; Y, Y^n | X = x) &= I(M; Y | X = x) + \underbrace{I(M; Y^n | Y, X = x)}_{\text{Equals 0 by Equation (37)}} \\ &= I(M; Y | X = x) \\ &= I_{\text{clean}}(x) \end{aligned} \tag{38}$$

- **Decomposition 2 (Grouping with Y^n):**

$$\begin{aligned} I(M; Y, Y^n | X = x) &= I(M; Y^n | X = x) + I(M; Y | Y^n, X = x) \\ &= I_{\text{noisy}}(x) + I(M; Y | Y^n, X = x) \end{aligned} \tag{39}$$

3. Final Derivation By equating Equation (38) and Equation (39), we have:

$$I_{\text{clean}}(x) = I_{\text{noisy}}(x) + I(M; Y | Y^n, X = x)$$

By the non-negativity property of mutual information, the final term must be non-negative:

$$I(M; Y | Y^n, X = x) \geq 0$$

Therefore, we conclude:

$$I_{\text{clean}}(x) \geq I_{\text{noisy}}(x) \quad \text{or} \quad \mathbf{I}_{\text{noisy}}(\mathbf{x}) \leq \mathbf{I}_{\text{clean}}(\mathbf{x})$$

Furthermore, the inequality is strict, $I_{\text{noisy}}(x) < I_{\text{clean}}(x)$, if $I(M; Y | Y^n, X = x) > 0$. This holds for any non-trivial noise channel $T(x)$ (i.e., not an identity or permutation matrix), as the noisy label Y^n becomes a statistically lossy proxy for the true label Y .

G. Experiment Details

G.1. Dataset Details

CIFAR-10/CIFAR-100 Both datasets consist of 50,000 training images. Following established conventions, we evaluate performance under three standard noise models:

- **Symmetric Noise:** Labels are randomly flipped to any of the other classes with a uniform probability.
- **Asymmetric Noise:** Labels are flipped to mimic real-world mistakes between visually similar categories (e.g., Horse \leftrightarrow Deer and Dog \leftrightarrow Cat).
- **Instance-Dependent Noise (IDN):** To approximate IDN without the prohibitive cost of a unique transition matrix for every sample, we use a grouped setting. The dataset is divided into 50 groups, with each group being assigned a different, randomly generated, diagonally-dominant transition matrix T .

We test a comprehensive range of noise levels: 20%, 50%, 80%, and 90% for symmetric noise, and 40% for asymmetric noise.

Clothing1M Clothing1M [55] is a large-scale, real-world benchmark for LNL. It contains 1 million images in 14 classes, crawled from online shopping websites. The dataset has a substantial level of intrinsic noise, estimated at approximately 38.5%.

G.2. Implementation Details

CIFAR-10/CIFAR-100 We use a PreActResNet-18 [21] backbone for all CIFAR experiments.

- **Standard Training:** The network is trained for 120 epochs using SGD with a weight decay of $5e-4$ and a batch size of 128. The initial learning rate is 0.02, decaying to 0.002 at 60 epochs and 0.0002 at 80 epochs.
- **Long Training (for Figure 1):** To observe the long-term collapse, we train for 800 epochs. The learning rate schedule is extended, decaying at 400 and 600 epochs.

Clothing1M Following the setup of [28], we use a ResNet-50 backbone pretrained on ImageNet. The network is trained for 150 epochs with a weight decay of $1e-3$ and a batch size of 32. The initial learning rate is 0.002, decaying by a factor of 10 at 50 and 100 epochs.

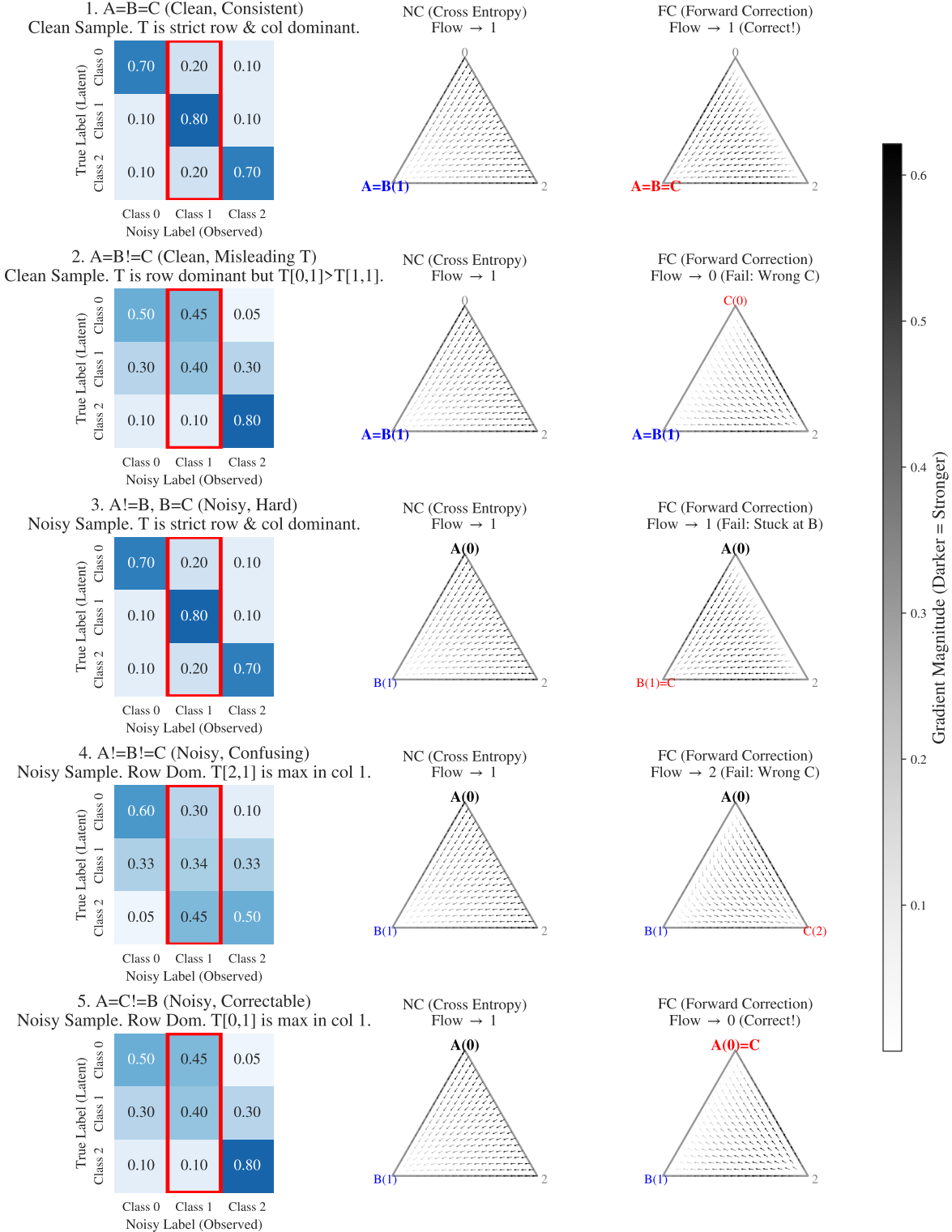


Figure 4. Gradient vector field of the FC loss on a 3-class simplex. We denote the clean label vertex as A (e_{y^*}), the noisy label as B (e_{y^n}), and the theoretical FC optimum as C ($e_{k_{FC}^*}$). The vector field confirms that the global minimum is at C . However, the noisy vertex B acts as a strong, non-optimal attractor. The vanishing gradient magnitude (“dead zone”) near B traps SGD, leading to the ‘pseudo-convergence’ analyzed in Section E.